Vol. 24, No. 3(2025) Bio25632
Revista Mexicana de Ingeniería Química

Kinetic and oxygen transfer assessment for Bikaverin production by *Gibberella fujikuroi*: Toward industrial scaling

Evaluación cinética y transferencia de oxígeno para la producción de bikaverina por *Gibberella fujikuroi:* Hacia el escalamiento industrial

D.B. Alanís-Gutiérrez[1], M.X. Negrete-Rodríguez[2], M.C. Chávez-Parga[3]*
[1,3]División de Estudios de Posgrado de la Facultad de Ingeniería Química, Universidad Michoacana de San Nicolás de Hidalgo, Santiago Tapia 403, Morelia Mich. 58000, México
[2]Tecnológico Nacional de México/Instituto Tecnológico de Celaya, García Cubas 600, Fovisste, Celaya, Gto., 38010, México
Sent date: July 16, 2025; Accepted: October 28, 2025

Abstract
Gibberella fujikuroi is a filamentous fungus that produces bikaverin, a pigment with pharmacological potential. Three strains (CDBB-H-972, CDBB-H-984 and CDBB-H-270) were evaluated in systems with forced aeration, analyzing the influence of pH and aeration rate. The CDBB-H-984 strain achieved the highest biomass concentration (15.73 ± 0.33 g/L at 48 h, pH 4, 0.5 vvm), while CDBB-H-972 presented the highest yield of bikaverin (0.134 ± 0.002 g bikaverin/g biomass at 96 h, pH 3, 0.75 vvm). The volumetric oxygen transfer coefficient (k_La) reached 169.90 ± 6.28 h^{-1} at 48 h and a maximum of 201.50 ± 2.42 h^{-1} at 72 h. The three-parameter Gompertz model described growth with high accuracy (R^2 = 0.999), while the Luedeking–Piret model confirmed that bikaverin is a metabolite not associated with growth. Bikaverin was purified and characterized by FT-IR, and morphology was evaluated by scanning electron microscopy. The Box–Behnken design indicated that the highest production of bikaverin was obtained with the CDBB-H-972 strain at pH 3 and an aeration rate of 1 vvm. Under these conditions, the oxygen consumption rate (OUR) exceeded the transfer rate (OTR), highlighting the need to increase aeration in larger-scale systems.
Keywords: Secondary metabolites, Bikaverin, Mass transfer, Biomass, Kinetic.

Resumen
Gibberella fujikuroi es un hongo filamentoso productor de bikaverina, un pigmento con potencial farmacológico. Se evaluaron tres cepas (CDBB-H-972, CDBB-H-984 y CDBB-H-270) en botellas con aireación forzada para estudiar la influencia del pH y la tasa de aireación. La cepa CDBB-H-984 alcanzó la mayor biomasa (15.73 ± 0.33 g/L a 48 h, pH 4, 0.5 vvm), mientras que CDBB-H-972 presentó el mayor rendimiento de bikaverina (0.134 ± 0.002 g/g biomasa a 96 h, pH 3, 0.75 vvm). El coeficiente volumétrico de transferencia de oxígeno (k_La) fue de 169.90 ± 6.28 h^{-1} a las 48 h y 201.50 ± 2.42 h^{-1} a las 72 h. El modelo de Gompertz de tres parámetros describió con precisión el crecimiento (R^2 = 0.999), y el modelo de Luedeking–Piret confirmó que la bikaverina es un metabolito no asociado al crecimiento. La bikaverina purificada se caracterizó por FT-IR, y la morfología se evaluó mediante microscopía electrónica de barrido. El diseño Box–Behnken indicó que la mayor producción es con la cepa CDBB-H-972 a pH 3 y 1 vvm. Bajo estas condiciones, la tasa de consumo de oxígeno (OUR) supera a la de transferencia (OTR), resaltando la necesidad de aumentar la aireación al escalar el proceso.
Palabras clave: Metabolitos secundarios, Bikaverina, Transferencia de masa, biomasa, Cinética.

*Corresponding author. *E-mail*: cparga@umich.mx;
https://doi.org/10.24275/rmiq/Bio25632
ISSN:1665-2738, *issn-e*: 2395-8472

1 Introduction

Bikaverin is a polyketide composed of 20 carbons, 14 hydrogens, and 8 oxygens. This compound exhibits a reddish pigment; therefore, its identification in submerged culture fermentation is immediate. In recent decades, several studies have reported its therapeutic properties, including antibiotic activity (Balan *et al*., 1970), antitumor activity (Hinojosa-Ventura *et al*., 2019), and neuroprotective activity (Nirmaladevi *et al.*, 2014).

Several authors have stated that bikaverin is widely found in fungal microorganisms of the genus *Gibberella fujikuroi*, which is known for producing secondary metabolites, primarily gibberellic acid (GA_3), including certain mycotoxins, including moniliformin, beauvericin, fusarins, fumonisins, fusaric acid, neurosporaxanthin, and bikaverin. However, the biosynthesis of bikaverin is strongly influenced by growth-related factors, such as the bioavailability of nutrients in the culture medium. Its production responds to nitrogen limitation and pH variations (Limón *et al*., 2010), as well as to a continuous air supply that promotes the biosynthesis of bikaverin (Giordano & Domenech, 1999).

Oxygen transfer often represents a major limitation in aerobic bioprocesses because of the inherently low solubility of oxygen in liquid media, making adequate aeration essential for fungal fermentations (Amaral *et al*., 2008). Industrial production of these secondary metabolites is typically carried out using mycelial cultures under submerged fermentation. Kinetic models describing fungal growth and secondary metabolite production, based on the physiological characteristics of the mycelium, have a significant influence on understanding, designing, and controlling industrial fermentation processes (Bailey & Ollis, 1977).

This study proposes the use of a fermentation system coupled with a forced-aeration mechanism to assess the influence of aeration rate (vvm) and pH on three different *G. fujikuroi* strains, applying the statistical criteria of a Box–Behnken experimental design and kinetic modeling of the fermentation process, with the aim of providing methodological bases to facilitate industrial scale-up of bikaverin production.

2 Materials and methods

2.1 Strains and inoculum preparation

In this study, *G. fujikuroi* strains CDBB-H-270, CDBB-H-972, and CDBB-H-984 (Colección de Cultivos del Departamento de Biotecnología y Bioingeniería, CINVESTAV-IPN, México) were used. The strains were maintained on Potato Dextrose Agar (Bioxon®) at 4 °C and subcultured monthly. The mycelium of *G. fujikuroi* was obtained from maintenance cultures grown on Potato Dextrose Agar (Bioxon®) incubated at 28 ± 1 °C for five days until full mycelial development. Subsequently, the fully developed mycelial material was recovered by adding 20 mL of sterile isotonic solution and homogenized using a sterilized serological pipette. The resulting homogenate was used as inoculum in 250 mL Erlenmeyer flasks containing 100 mL of liquid culture medium composed of dextrose (30 g/L) as the carbon source, NH_4NO_3 (1.2 g/L) as the nitrogen source, mineral salts KH_2PO_4 (5.09 g/L), $MgSO_4{\cdot}7H_2O$ (1.091 g/L), and trace elements (2 mL/L). Incubation was carried out on an orbital shaker using Erlenmeyer flasks (LabTech®) at 250 rpm and 28 ± 1 °C for 38 ± 2 h.

2.2 Culture medium and cultivation conditions

The maximum biomass formation and bikaverin production of the three *G. fujikuroi* strains were evaluated in a culture medium containing anhydrous dextrose (REPROQUIFIN®) as the carbon source, NH_4Cl (REPROFIQUIN®) as the nitrogen source, KH_2PO_4 (Golden Bell®) as the phosphate source, and a trace-element solution. Fermentations were conducted in GL45 Kimax® bottles equipped with a cylindrical stainless-steel diffuser (2 μm pore size). Each bottle was inoculated with 10 % (v/v) of a homogenized mycelial suspension (30 mL inoculum in 300 mL of medium) and incubated for 96 hours under orbital agitation at 100 rpm and 28 ± 1 °C.

The culture medium was freshly prepared prior to each fermentation experimental treatment, and all components were sterilized at 121 °C for 15 min in an autoclave (HMC EUROPE HV-50L©). The air supply was sterilized by passage through a 0.45 μm PVDF membrane prior to sparging. All glassware, tubing, and fittings were autoclaved before assembly, and the diffusers were disinfected with 70 % ethanol before each fermentation. These procedures ensured that aseptic conditions were maintained throughout the experimental process.

2.3 Experimental design (Box–Behnken)

A Box–Behnken response surface design was employed to simultaneously evaluate the effects of strain, pH, and aeration rate on biomass and bikaverin production (Table 1). The inclusion of the strain as a factor was based on the biosynthetic variability among *G. fujikuroi* isolates, which can influence their response to cultivation conditions. The coded values -1, 0, and 1 correspond to the low, medium, and high levels of each

Table 1. Parameters and levels used in the Box–Behnken experimental design.

Independent variables	Symbol	Coded levels		
		-1	0	1
Strain	C	CDBB-H-270	CDBB-H-972	CDBB-H-984
Aeration rate (vvm)	A	0.5	0.75	1
pH	pH	3	4	5

factor, respectively, as established in the experimental design.

The experimental setup followed a Box–Behnken design to assess the effects of pH, aeration rate, and fungal strain on bikaverin biosynthesis by *G. fujikuroi*. The experimental treatments were randomized using Minitab 19 ® software to minimize systematic errors and ensure statistical independence among treatments. Each treatment was performed in triplicate, and all data are reported as mean ± standard deviation.

The response variables were dry biomass (g/L) and bikaverin concentration (mg/L). The design included fifteen treatments with three replicates at the central point, randomized to minimize bias. The fitted quadratic model is expressed in Equation (1):

$$Y = \beta_0 + \beta_1 C_1 + \beta_2 pH_2 + \beta_3 A_3 + \beta_{11} C_1^2 + \beta_{22} pH_2^2 + \beta_{33} A_3^2 + \beta_{12} C_1 pH_2 + \beta_{13} C_1 A_3 + \beta_{23} pH_2 A_3 \quad (1)$$

where Y corresponds to the biomass or bikaverin concentration, C to the strain, A to the aeration rate (vvm), and pH to the coded pH values, the coefficients β represent the estimated regression parameters.

Statistical analysis was performed using Minitab 19® software through ANOVA ($\alpha = 0.05$). Based on the fitted models, response surface plots were constructed. The time course of biomass and bikaverin production was determined by measuring the samples at 0, 24, 48, 72, and 96 hours for each cultivation condition.

2.4 *Analysis of pH on biomass production*

To examine how variations in pH influence the growth behavior of *G. fujikuroi*, the experimental treatments corresponding to the three pH levels of the Box–Behnken design were analyzed using strain CDBB-H-972, selected for its intermediate and representative behavior compared to the other isolates. This approach allowed isolating the effect of pH as the variable of interest by reducing the variability attributable to genetic differences among strains and reinforcing its relevance under optimized cultivation conditions.

The medium pH was adjusted to 3, 4, and 5 using 1 N HCl or 1 N NaOH prior to inoculation. During cultivation, samples were taken at 0, 24, 48, 72, and 96 h. Aliquots of 1 mL were collected for pH measurement using a previously disinfected electrode (HANNA®) connected to a potentiometer (Thermo Fisher Scientific® Orion Star A2114). For biomass determination, 10 mL samples were taken, filtered under vacuum, and dried in an oven to constant weight. The statistical assessment of pH influence on biomass production involved a one-way ANOVA followed by Tukey's honestly significant difference (HSD) test at a confidence level of 95%.

2.5 *Analysis of aeration rate on* bikaverin production

To elucidate the relationship between aeration and bikaverin productivity in *G. fujikuroi*, experimental treatment 12 from the Box–Behnken design was selected, corresponding to the condition that yielded the highest pigment concentration. In this experimental treatment, the dynamic method described by Doran (2013) was applied, a widely used approach for estimating the volumetric oxygen transfer coefficient (k_La) and the oxygen transfer rate (OTR).

The dissolved oxygen (DO) concentration was measured using a digital probe (Smart Sensor AR8406®), which records data at 10-second intervals corresponding to the sensor's response time. A minimum of 30 data points per curve was obtained to ensure adequate statistical fitting. The OTR was defined according to Equation (2):

$$OTR = k_La\left(C^*_{0_2} - C_{O_2}\right) \quad (2)$$

where OTR is the oxygen transfer rate in the system ($mg\ O_2/Lh$), k_La is the mass transfer coefficient (h^{-1}), $C^*_{0_2}$ is the oxygen concentration at the gas–liquid interface (mg / L); and C_{O_2} is the oxygen concentration within the liquid phase (mg / L).

The oxygen uptake rate (OUR) was calculated according to Equation (3):

$$OUR = Q_{O_2}X \quad (3)$$

where OUR is the oxygen consumption by the microorganism ($mg\ O_2/Lh$), Q_{O_2} is the specific oxygen consumption rate per unit of biomass and time ($mg\ O_2/Lh$) and X is the biomass concentration (g/L). It is essential to note that the term aeration rate (vvm) refers to the supplied airflow, distinguishing it from the agitation speed (rpm) to avoid conceptual ambiguities.

2.6 Biomass production kinetics

The growth dynamics of *G. fujikuroi* were evaluated under the optimal pH and aeration rate conditions determined by the Box–Behnken design. To describe microbial growth, three kinetic models were used: the two-parameter Gompertz model, the modified three-parameter Gompertz model, and the Logistic model. The specific growth rate $\left(\mu,\ h^{-1}\right)$ was calculated from the slope of biomass values in 24-hour intervals according to Equation (4):

$$\mu = \frac{\ln\left(\frac{X_2}{X_1}\right)}{t_2 - t_1} \tag{4}$$

In this expression, X_1 and X_2 denote biomass concentrations (g/L) measured at times t_1 and t_2 (s) respectively. Generally, microbial growth models can be formulated with or without coupling to substrate consumption and usually include two or three adjustable parameters. The mathematical models considered here, which are independent of substrate consumption, are presented in Equations (5) – (7).

$$\frac{dX}{dt} = kXe^{-\mu t} \tag{5}$$

$$\frac{dX}{dt} = kXe^{-\mu t} - aX \tag{6}$$

$$\frac{dX}{dt} = kX - aX^2 \tag{7}$$

where X is the generated biomass (g/L), a and k are kinetic constants. Equation (5) corresponds to the two-parameter Gompertz model, Equation (6) to the three-parameter Gompertz model, and Equation (7) describes the Logistic model. Equations (5) – (7) were integrated using Python programming language.

Model comparison was performed using an F-test under the assumption that the three-parameter model predicts biomass precisely at each time point, as shown in Equation (8):

$$f = \frac{\frac{(RSS_2 - RSS_1)}{(DF_2 - DF_1)}}{\frac{RSS_1}{DF_1}} \tag{8}$$

where RSS_2 is the residual sum of squares of the Logistic model, RSS_1 is the residual sum of squares of the Gompertz model, DF_1 is the number of degrees of freedom of the Logistic model, and DF_2 is the number of degrees of freedom of the Gompertz model. The calculated f value was compared with the corresponding value from the F distribution table. Likewise, a comparison was made between the three-parameter Gompertz and Logistic models. If f is lower than F, no additional parameter is required; if f exceeds F, a different model must be selected. This analysis is an approximation due to the comparison of nonlinear models for model discrimination (Zwietering *et al.*, 1990).

2.6.1 Product formation kinetics

Bikaverin synthesis was evaluated using the Luedeking–Piret model, which describes product formation as the sum of a growth-associated and a non-growth-associated fraction, as defined in Equation (9):

$$\frac{dP}{dt} = \alpha\frac{dX}{dt} + \beta X \tag{9}$$

where P is the product concentration (g/L), X is the biomass concentration (g/L), α is the growth-associated formation coefficient, and β is the non-growth-associated formation coefficient. Thus, high α values indicate that bikaverin production depends mainly on cell growth, whereas high β values reflect a synthesis that is independent of growth.

2.7 Analytical determinations

Every 24 h, over a period of 96 h, subsamples of 11 mL were taken from the culture. From this volume, 10 mL were used for dry biomass determination by vacuum filtration using 0.45 μm membranes (Advantec®), followed by oven drying at 95 °C until constant weight was achieved. From the obtained filtrate, 1 mL was used for the analytical determination of medium components. Total reducing sugars (TRS) were quantified using the DNS method (Miller, 1959), and ammoniacal nitrogen was determined using the Berthelot method (Solórzano, 1969). Absorbance readings were performed on a UV–Vis spectrophotometer (Evolution 350, Thermo Fisher Scientific®).

The remaining 1 mL of each subsample was used to monitor mycelial growth by optical microscopy, allowing for the recording of morphological changes throughout the cultivation process.

2.8 Extraction and analysis of bikaverin production

An aliquot of the crude bikaverin extract was subjected to liquid–liquid partitioning with chloroform. Subsequently, separation was performed by glass column chromatography (36 cm height × 1.5 cm internal diameter), using silica gel 60 impregnated with oxalic acid (95:05, w/w) as the stationary phase. The mobile phase consisted of a mixture of chloroform:methanol:acetic acid (94:1:5, v/v/v). The collected fractions were monitored by normal-phase thin-layer chromatography (TLC) by comparing the obtained spots with a bikaverin standard (Sigma-Aldrich®). The positive fractions were concentrated and subsequently precipitated with methanol at –70 °C for 24 h, yielding pure bikaverin in crystalline form.

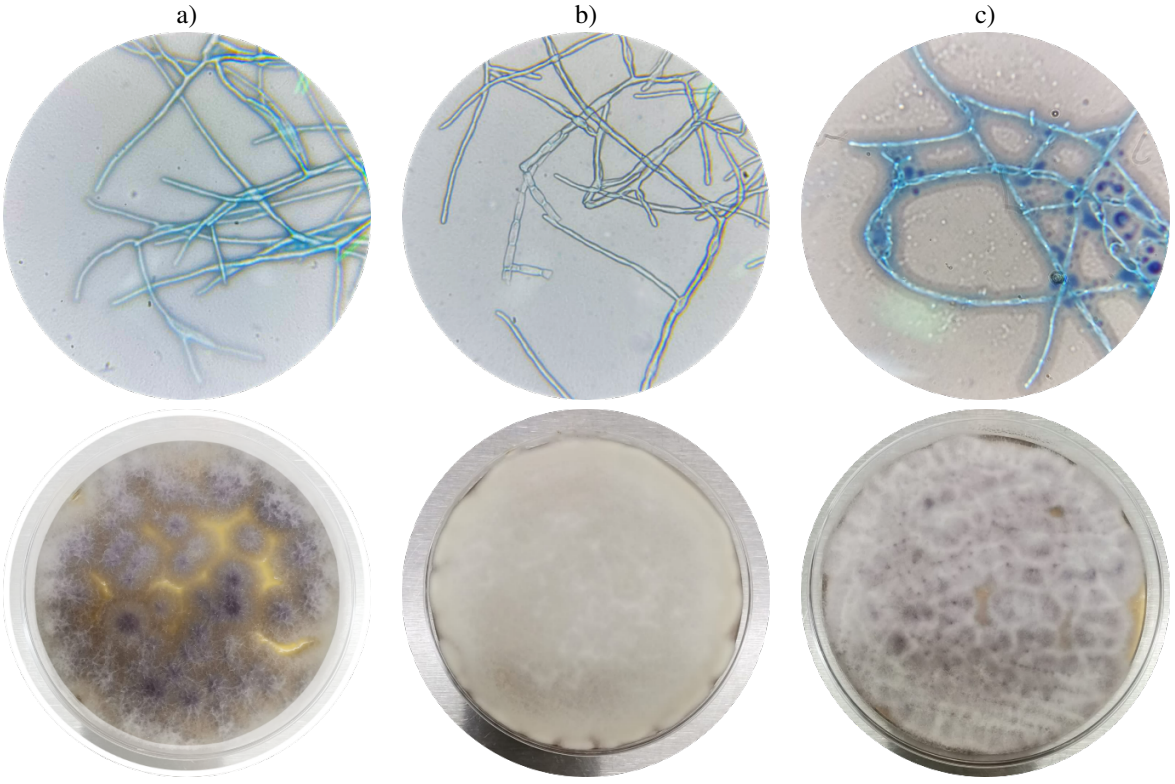

Figure 1. *G. fujikuroi* strains cultivated in liquid and solid media, stained with lactophenol blue. Submerged mycelium of strains a) CDBB-H-984, b) CDBB-H-972, and c) CDBB-H-270 grown in liquid medium and observed under an optical microscope at 100× magnification using an oil-immersion objective; the lower panels show the corresponding aerial mycelium of each strain grown on solid surfaces.

2.8.1 Structural and morphological characterization

The structural characterization of bikaverin was carried out by Fourier-transform infrared spectroscopy (FTIR) using a Spectrum 400 spectrometer (Perkin-Elmer®). Spectra were obtained in the range of 4000–800 cm^{-1} with a spectral resolution of 4 cm^{-1}, employing the MIR mode and four scans per sample.

For the morphological study, subsamples corresponding to different cultivation times were analyzed. Fresh material was observed using microscopy (LABOMED®) without staining, using a 100× objective lens. Additionally, the dehydrated material was examined by using scanning electron microscopy (SEM) with a JEOL JSM-7600F® instrument (Institute of Metallurgy and Materials, UMSNH).

3 Results and discussion

3.1 Strains

After five days of incubation at 28 ± 1 °C, a fully developed mycelium was observed in the three *G. fujikuroi* strains (Figure 1). In the optical micrographs (100×, stained with lactophenol blue), characteristic fungal structures such as conidia and chlamydospores were distinguished.

The CDBB-H-270 strain exhibited thicker hyphae and a more intense staining, associated with an advanced maturation state. In contrast, strains CDBB-H-972 and CDBB-H-984 showed thinner hyphae and cell walls with less pronounced thickening, characteristics of an actively growing mycelium. On solid medium, strain CDBB-H-984 displayed a more pronounced reddish pigmentation associated with bikaverin production, whereas CDBB-H-972 presented a predominantly white mycelium, and CDBB-H-270 exhibited a rough surface growth with lower homogeneity.

These morphological differences reflect the physiological variability among isolates, a phenomenon widely reported in species of the *Fusarium* genus, where genetic diversity has been documented to manifest in morphological changes, growth rate, and secondary metabolite production (Leslie & Summerell, 2006; Anama *et al*., 2021; Martínez-Moreno *et al*., 2021). However, these differences do not always correlate with productivity in submerged culture, as observed in this study with strain CDBB-H-270, which showed lower biomass and pigment yields. Overall, the observed variability justifies the inclusion of the strain as a factor in a comprehensive analysis such as the

Table 2. Bikaverin production (mg/L) by three *G. fujikuroi* strains under each experimental condition defined by the Box–Behnken response surface design. Values represent the mean ± standard deviation (n = 2).

Experimental treatment	Strain	Aeration rate (vvm)	pH	Bikaverin production (mg/L) 96 hours
1	972	0.75	4	331.25 ± 0.18
2	270	1.00	4	30.57 ± 0.77
3	270	0.75	5	86.75 ± 1.39
4	984	1.00	4	30.07 ± 0.92
5	972	0.50	3	483.58 ± 2.28
6	984	0.75	3	80.07 ± 6.30
7	270	0.75	3	88.65 ± 3.98
8	984	0.50	4	33.98 ± 1.61
9	972	0.75	4	345.45 ± 0.86
10	270	0.50	4	83.68 ± 2.56
11	984	0.75	5	73.53 ± 4.67
12	972	1.00	3	930.44 ± 6.95
13	972	1.00	5	40.59 ± 3.49
14	972	0.50	5	77.81 ± 5.85
15	972	0.75	4	339.90 ± 1.66

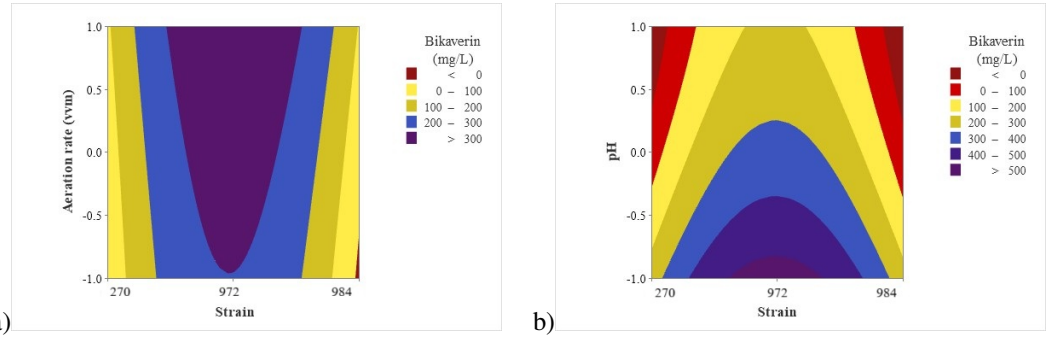

Figure 2. Response surface contour plots for bikaverin production: (a) strain × aeration interaction (pH fixed at 0; pH = 4); (b) strain × pH interaction (aeration fixed at 0; aeration = 0.75 vvm).

Box–Behnken design, reinforcing the influence of genetic factors on biomass and bikaverin production (Limón *et al*., 2010).

3.2 *Analysis of the Box–Behnken response surface design*

The Box–Behnken experimental design allowed the simultaneous evaluation of the effects of strain, pH, and aeration rate on bikaverin production. Fifteen experimental treatments were carried out according to the planned matrix (see Table 2). Under all experimental conditions, the highest bikaverin production was observed at 96 h of cultivation; therefore, this point was selected to fit the response surface model.

According to the Box–Behnken design results (Table 2), bikaverin production was markedly influenced by the strain factor, with *G. fujikuroi* CDBB-H-972 showing the highest pigment yields compared with isolates CDBB-H-270 and CDBB-H-984. The maximum concentration (930.44 ± 6.95 mg/L) was obtained with this strain at an aeration rate of 1.0 vvm and an initial pH of 3, suggesting that moderate aeration combined with acidic conditions favors secondary metabolite biosynthesis.

In contrast, the other isolates exhibited significantly lower production under similar conditions (< 100 mg/L), confirming the strain-dependent variability commonly reported for *G. fujikuroi* and other bikaverin-producing fungi. Aeration and pH also showed interactive effects, where higher oxygen transfer (1.0 vvm) at neutral to slightly acidic pH promoted growth but did not necessarily enhance pigment accumulation, consistent with the non-growth-associated nature of bikaverin synthesis.

The response surface plots (Figure 2) show that strain CDBB-H-972 is the most favorable for bikaverin production. In the strain × aeration interaction (Figure 2a), the highest pigment concentration was obtained with strain CDBB-H-972 even at low aeration rates (≥ 0.75 vvm).

Table 3. Analysis of variance (ANOVA) of the response surface model for biomass formation. F: Fisher's test; P: significance test. Significance levels: $\alpha = 0.05$ and $\alpha = 0.1$.

Source	DF	Adjusted SS	Adjusted MS	*F-value*	*p-value*
Model	9	631794	70199	1.50	0.342
Linear	3	228762	76254	1.63	0.296
Strain	1	648	648	0.01	0.911
Aeration rate	1	15543	15543	0.33	0.590
pH	1	212572	212572	4.53	**0.087**
Quadratic	3	343838	114613	2.44	0.179
Strain*Strain	1	326953	326953	6.97	**0.046**
Aeration rate*Aeration rate	1	40	40	0.00	0.978
pH*pH	1	6194	6194	0.13	0.731

In contrast, strains CDBB-H-270 and CDBB-H-984 did not reach high production levels under any aeration conditions. In the strain × pH interaction (Figure 2b), the optimum was observed with strain CDBB-H-972 at an approximate pH of 3, where bikaverin values above 400 mg/L were achieved; as the pH increased toward more neutral values (pH = 5), production decreased significantly.

Experimental treatment 12 (strain CDBB-H-972, pH 3, aeration 1.0 vvm) showed the highest concentration observed in this study (930.44 mg/L), confirming that this combination of conditions is favorable for maximizing pigment synthesis. This finding is consistent with optimizations reported in other polyketide-producing fungi, such as *Fusarium oxysporum*, where response surface methodology was used to optimize bikaverin production in flasks (Santos *et al.,* 2020). Furthermore, the ability of *G. fujikuroi* to modulate secondary metabolite biosynthesis under environmental variations has been recently documented, for example, in studies addressing nitrogen availability and its effect on the simultaneous production of bikaverin and gibberellins (Giordano, 1999).

The relevance of the strain factor is consistent with the notion that intrinsic physiological variability among isolates may exert a greater influence than minor operational factors, a phenomenon highlighted in recent works on the regulation of polyketide pigments in fungi (Lu *et al*., 2025). The analysis of variance (ANOVA) of the fitted model (Table 3) revealed that the linear pH term was statistically significant at a level of $\alpha = 0.05$ (*p-value* = 0.087, close to the threshold), indicating that pH variation affects bikaverin production. Moreover, the quadratic term associated with the strain (strain²) was significant (*p-value* = 0.046) when a significance level of $\alpha = 0.1$ was considered, suggesting that the effect of the strain is not linear and that there is an optimal response dependent on its intrinsic condition.

The analysis of variance (Table 3) indicates that the response surface model explained the observed variation in bikaverin production, although not all factors were significant at the $\alpha = 0.05$ level. The pH showed a near-significant effect ($p = 0.087$), confirming its critical influence on pigment biosynthesis. Likewise, the quadratic term associated with the strain was significant ($p = 0.046$), demonstrating that the variability among isolates does not follow a strict linear pattern but rather presents an optimum linked to the strain's physiology. In contrast, aeration did not show a statistically significant effect under the conditions evaluated ($p = 0.590$). However, graphical results suggest that an airflow higher than 0.5 vvm is required to maintain adequate pigment levels.

In summary, the results of the Box–Behnken design indicate that strain CDBB-H-972 and acidic conditions favor bikaverin production, justifying a more detailed analysis of the individual effects of pH and aeration, which is developed in the following sections.

3.3 Effect of pH on biomass production

Figure 3 shows the biomass generation in the *G. fujikuroi* CDBB-H-972 strain grown at three initial pH values (3, 4, and 5). It was observed that treatment at pH 5 promoted greater biomass accumulation compared to pH 3 and pH 4, which presented similar values.

The statistical analysis confirmed that pH had a significant effect on the final biomass at 96 hours of fermentation (ANOVA, F (2,3) = 31.93, p = 0.010). Tukey's multiple comparison test showed that pH 5 resulted in significantly higher biomass (12.66 ± 0.11 g/L) than pH 3 (8.65 ± 0.77 g/L) and pH 4 (8.08 ± 0.75 g/L), whereas no significant differences were found between pH 3 and pH 4 (Table 4).

These results suggest that a less acidic medium (pH = 5) favors biomass accumulation in *G. fujikuroi*. However, bikaverin synthesis is more closely associated with acidic values, since the bik genes responsible for its biosynthesis are only expressed under such conditions (Medentsev *et al*., 2005; Wiemann *et al*., 2009). Previous studies have shown that the progressive decrease in pH favors the bikaverin metabolic pathway: Giordano and Domenech (1999) reported that in

Table 4. Effect of pH on the biomass of *G. fujikuroi* CDBB-H-972 at 96 h. Values correspond to the mean ± standard deviation (n = 2). Significant differences between means were identified using Tukey's test (different letters indicate significant difference, $\alpha = 0.05$).

Source	DF	Adjusted SS	Adjusted MS	*F-value*	*p-value*
pH	2	24.841	12.421	31.930	0.010
Error	3	1.1670	0.389	-----	
Total	5	26.008	------	-----	
pH	Mean Biomass (g/L) ± DE		Tukey group		
3	8.65 ± 0.77		**a**		
4	8.08 ± 0.75		**a**		
5	12.66 ± 0.11		**b**		

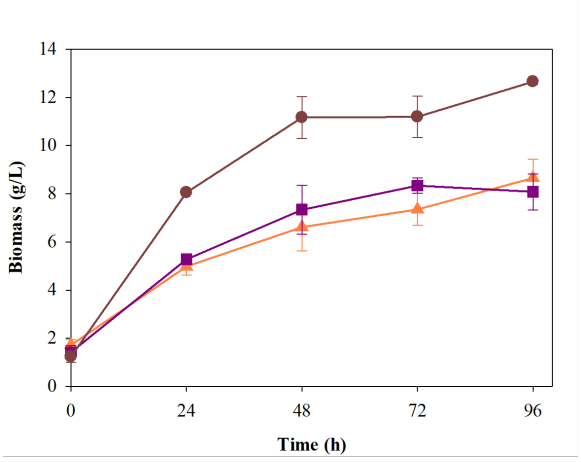

Figure 3. Effect of initial pH on biomass generation (g/L) of *G. fujikuroi* CDBB-H-972 during 96 hours of fermentation. Data represents mean values ± standard deviation (n = 2 biological replicates). [pH = 3 ▲, 0.5 vvm; pH = 4 ■, 0.75 vvm; pH = 5 ●, 1.00 vvm].

F. fujikuroi, an initial pH of 4.5 that decreased to 3.7 during fermentation promoted maximum pigment production. Similarly, Santiago (2013) described that in *Fusarium decemcellulare*, maximum pigmentation occurred between 48 and 72 hours, an interval consistent with the observations in this study.

Overall, these results confirm the dual role of pH in *G. fujikuroi*: neutral or slightly acidic values (pH 5) favor mycelial growth, whereas more acidic conditions (pH 3 – 4) are critical for the activation of bikaverin biosynthetic pathways.

In summary, the obtained results demonstrate that the initial pH is a crucial factor in determining biomass accumulation in *G. fujikuroi*, as it promotes mycelial growth under less acidic conditions. However, it does not necessarily promote pigment synthesis. Considering that bikaverin production depends not only on the physiological state of the fungus but also on the availability of dissolved oxygen in the medium, it becomes essential to evaluate the effect of aeration as a critical variable in the bioprocess. The following section presents the results of oxygen transfer analysis and its relationship with bikaverin accumulation, based on the experiments from the Box–Behnken design.

3.4 *Effect of aeration rate on bikaverin production*

Figure 4 shows the dissolved oxygen profiles during the fermentation of *G. fujikuroi* CDBB-H-972 at different cultivation times (0, 24, 48, 72, and 96 h), while Table 5 summarizes the calculated oxygen transfer and consumption parameters. At 0 h, the k_La value was 59.08 ± 4.75 h^{-1}, with a specific oxygen consumption rate (QO_2) of 79.02 ± 2.56 mg O_2/g*h and an OUR of 100.66 ± 2.87 mg O_2/g*h, reflecting a system not yet limited by oxygen due to the low biomass present.

At 24 h, the k_La increased to 79.55 ± 1.60 h^{-1}; however, the OUR (514.43 ± 41.07 mg O_2/L*h) exceeded the OTR (467.50 ± 42.92 mg O_2/L*h), indicating an imbalance between cellular demand and transfer capacity. This behavior intensified at 48 h, when a k_La of 169.90 ± 6.28 h^{-1} and an OUR of 1039.49 ± 25.59 mg O_2/L*h was recorded, confirming that the system was under oxygen-limiting conditions, coinciding with the phase of highest metabolic activity. Subsequently, at 72 h, the maximum k_La value (201.50 ± 4.22 h^{-1}) was reached, and the OUR also remained high (1287.94 ± 13.97 mg O_2/L*h).

Table 5. Correlation results of k_La, QO_2, OTR, OUR, and bikaverin production from the initial time (0 h) to 96 h of fermentation, during the fermentation of *G. fujikuroi* CDBB-H-972, pH = 3.

Time (h)	k_La (h^{-1})	Q_{O_2} (mg O_2)/(g*h)	OTR (mg O_2)/(L*h)	OUR (mg O_2/L*h)	Bikaverin (mg/L)	R^2
0	59.08 ± 4.75	79.02 ± 2.56	87.19 ± 0.41	100.66 ± 2.87	5.93 ± 1.09	0.867
24	79.55 ± 1.60	99.90 ± 1.15	467.50 ± 42.92	514.43 ± 41.07	30.69 ± 11.76	0.946
48	169.90 ± 6.28	135.56 ± 2.78	1003.95 ± 26.32	1039.49 ± 25.59	43.71 ± 15.74	0.944
72	201.50 ± 2.42	154.05 ± 1.99	1262.05 ± 14.01	1287.94 ± 13.97	180.81 ± 24.21	0.873
96	112.88 ± 2.03	85.12 ± 17.66	662.19 ± 12.08	690.37 ± 11.55	931.77 ± 22.13	0.935

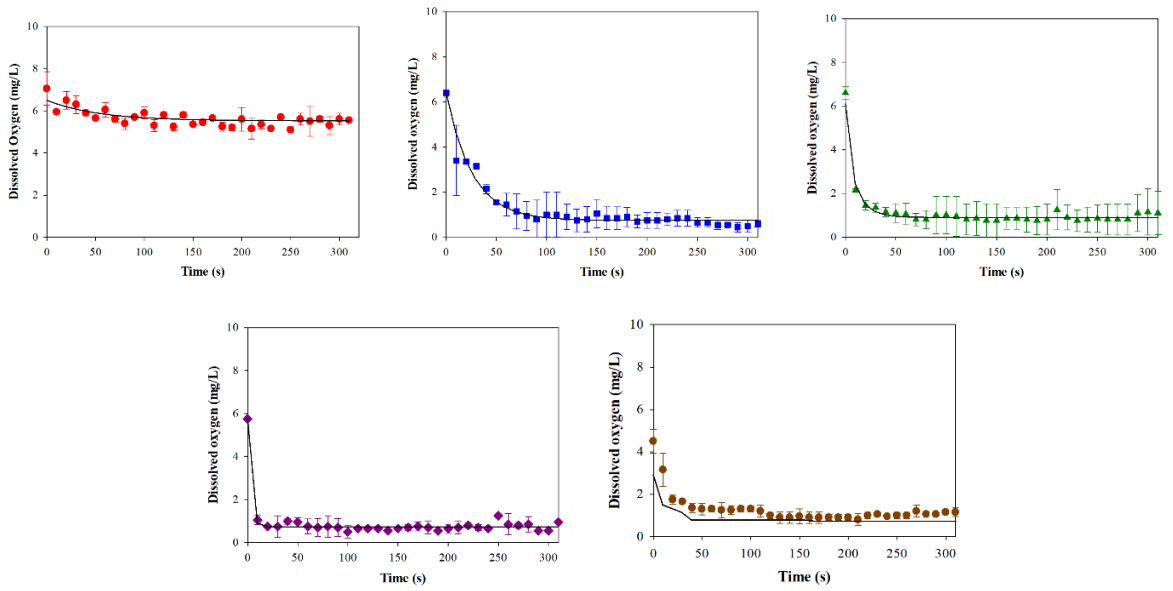

Figure 4. Dissolved oxygen (DO) profiles during the fermentation of *G. fujikuroi* CDBB-H-972, pH = 3 at different sampling times: 0 h (●), 24 h (■), 48 h (▲), 72 h (♦), and 96 h (⬟). The curves represent the fit obtained using the dynamic method for the calculation of k_La. A progressive decrease in dissolved oxygen concentration is observed as the culture proceeds, indicating that metabolic demand exceeds the transfer capacity during intermediate stages (24 - 48 h), generating oxygen-limiting conditions associated with bikaverin production.

However, bikaverin accumulation increased significantly (180.81 ± 24.21 mg/L), suggesting that oxygen limitation may have acted as a stimulus for the biosynthesis of this secondary metabolite. Finally, at 96 h, although the k_La decreased to 112.88 ± 2.03 h^{-1} and the OUR was reduced to 690.37 ± 11.55 mg O_2/L*h, bikaverin production reached its maximum (931.77 ± 22.13 mg/L). This suggests that pigment synthesis occurs preferentially under conditions of lower respiratory demand, a typical feature of intracellular metabolite accumulation (Giordano & Domenech, 1999; Wiemann *et al.,* 2009).

Overall, the results confirm that the OTR/OUR dynamics play a determining role in the fermentation process and that progressive oxygen limitation is a key factor in the induction of the bikaverin biosynthetic pathway.

In this study, it was observed that the relationship between the oxygen uptake rate (OUR) and the oxygen transfer rate (OTR) was strongly associated with bikaverin production. During the first 48 h, the OUR exceeded the OTR, indicating that the limiting conditions coincided with high metabolic activity. Subsequently, at 72–96 h, although k_La values fluctuated, bikaverin production increased significantly, supporting the hypothesis that oxygen limitation can act as a stimulus for secondary metabolite synthesis (Giordano & Domenech, 1999; Wiemann *et al.,* 2009).

Consistently, Chávez-Parga *et al.* (2014) reported that increasing aeration and agitation enhanced k_La values in an STR bioreactor, achieving favorable conditions for bikaverin production, although with a critical balance between oxygenation and mechanical stress on the mycelium. These findings align with recent reviews that recognize oxygen transfer as a primary challenge in the large-scale production of filamentous fungi, having a dual effect: promoting initial growth but inducing secondary pathways under limitation (Spraker *et al.*, 2018; Machado *et al.*, 2022). In this context, the results suggest that aeration strategies should not only aim to maximize k_La but also allow controlled limitation periods that favor intracellular bikaverin accumulation.

Comparable results have been recently reported in non-conventional biosaccharification and fermentation processes, where the selection of native strains and operational conditions were key to maximizing productivity (Garza-Garza *et al.*, 2025). This reinforces the importance of considering critical operational variables such as aeration and pH in the optimization of fungal bioprocesses. From a bioprocess perspective, the results obtained under forced aeration highlight the potential for process scale-up to industrial systems. The higher oxygen transfer coefficients (k_La) and bikaverin yields observed in aerated cultures suggest that similar performance could be achieved in external-loop airlift bioreactors. These systems offer efficient gas–liquid mass transfer and mixing with lower energy consumption compared to conventional stirred-tank reactors, which is a critical advantage for large-scale pigment production. Such scalability considerations are consistent with previous reports describing the influence of aeration and hydrodynamics on fungal secondary metabolism and bioreactor performance

(Limón *et al*., 2023; Chisti, 2016).

Taken together, the results obtained for the effects of pH and aeration on biomass and bikaverin production confirm that the cultivation conditions directly influence the activation of specific metabolic pathways. While pH determined the chemical environment favorable for *bik* gene expression, oxygen transfer modulated the balance between primary and secondary metabolism, acting as a key limiting factor in the critical stages of the process. Nevertheless, these factors alone do not fully explain the production dynamics. Therefore, it is essential to address the overall kinetics of growth and product formation, which not only allows the identification of the mathematical model that best describes biomass generation but also establishes the coupling relationship between cell growth and bikaverin synthesis through the Luedeking–Piret model.

3.5 Bikaverin production kinetics

The growth and bikaverin production kinetics were evaluated under experimental conditions defined from the optimal treatment of the Box–Behnken design (experiment 12). In this assay, *G. fujikuroi* strain CDBB-H-972 was cultivated in a medium composed of dextrose (50 g/L), NH_4Cl (0.75 g/L), KH_2PO_4 (1 g/L), and $MgSO_4$ (1 g/L). The initial pH was adjusted to 3.0 using 1 N HCl or 1 N NaOH; temperature was maintained at 28 ± 1 °C, and orbital agitation at 100 rpm. Aeration was set at 1 vvm (0.3 L/min in a working volume of 300 mL), and the inoculum corresponded to 10% (v/v) of a 36-h pre-culture.

These conditions were selected because they represented the scenario with the highest bikaverin production within the experimental matrix. The culture evolution showed a typical submerged fermentation profile, with progressive consumption of total reducing sugars (TRS) and ammoniacal nitrogen, accompanied by biomass increase and intracellular bikaverin accumulation (Figure 5).

The fitting of experimental data to mathematical growth models (two-parameter Gompertz, three-parameter Gompertz, and Logistic) showed that all three adequately described the system dynamics (Figure 6). However, the three-parameter Gompertz model exhibited the highest goodness of fit (R^2 = 0.999), capturing more accurately the transition toward the stationary phase. This suggests that this model is more sensitive to initial biomass variations and better represents the slight decrease observed at the end of the culture, attributed to reserve consumption under limiting conditions (Borketas *et al*., 2025). Similarly, Valle *et al*. (2024) applied nonlinear mathematical models to describe the fermentation of *Torulaspora delbrueckii* and found that the three-parameter Gompertz model provided a better representation of growth and substrate consumption, which is consistent with the strategy employed in this study for modeling the kinetics of *G. fujikuroi*.

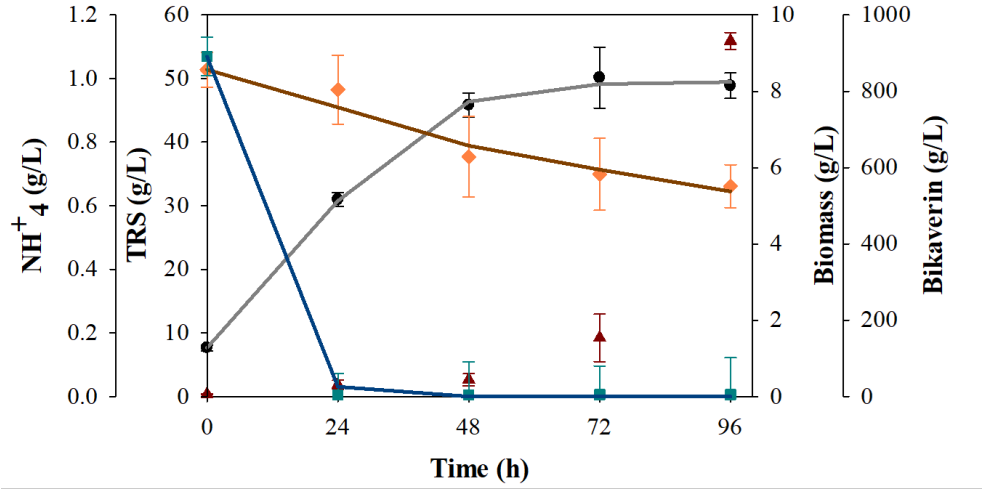

Figure 5. Fermentation kinetics of *G. fujikuroi* CDBB-H-972 under controlled conditions (dextrose 50 g/L, NH_4Cl 0.75 g/L, KH_2PO_4 1 g/L, $MgSO_4$ 1 g/L, initial pH 3, temperature 28 ± 1 °C, aeration 1 vvm, orbital agitation 100 rpm, inoculum 10% v/v). Evolution of biomass (•; fitted to the three-parameter Gompertz model), total reducing sugars, TRS (♦; fitted curve), ammoniacal nitrogen, NH_4^+ (■; fitted curve), and bikaverin concentration (▲) throughout 96 h of fermentation. Data represents the mean of two independent replicates ± standard deviation.

Table 6. Kinetic parameters obtained from biomass fitting to the Gompertz (two- and three-parameter) and Logistic models. Shown are the values of the growth constants (k, μ, and a), residual sum of squares (RSS), determination coefficient (R^2), and statistical model comparison using the F-test ($\alpha = 0.05$).

Model	Parameters			Yields	RSS	R^2	Comparison		
	k	μ	a	g/g					
Two-parameter Gompertz	0.110	0.058	-----	$Y_{\frac{X}{S}} = 0.3751 \pm 0.065$	0.114	0.996	**Models**	**F**	***p-value***
Three-parameter Gompertz	0.102	0.047	0.002	$Y_{\frac{P}{X}} = = 0.134 \pm 0.002$	0.003	0.999	Logistic vs G3P	29.840	0.031
Logistic	0.091	--------	0.011		0.049	0.998	G2P vs G3P	71.250	0.137

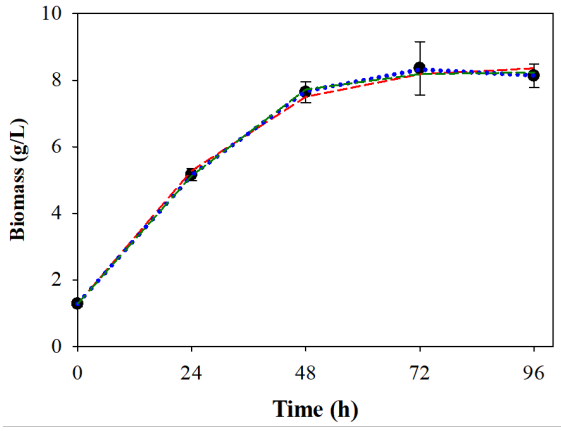

Figure. 6. Fitting of the growth kinetics of *G. fujikuroi* CDBB-H-972 during bikaverin production to three mathematical models: two-parameter Gompertz (- - -), three-parameter Gompertz (· · ·), and Logistic (- - -). Symbols represent the experimental data (●). Conditions: dextrose 50 g/L, NH_4Cl 0.75 g/L, KH_2PO_4 1 g/L, $MgSO_4$ 1 g/L, initial pH 3, 28 ± 1 °C, aeration 1 vvm, orbital agitation 100 rpm, inoculum 10% v/v.

Table 6 summarizes the kinetic parameters obtained and the statistical comparison between models using the F-test. Although both the Logistic and the two-parameter Gompertz models showed acceptable fits ($R^2 > 0.999$), the F-test indicated significant differences between the Logistic and the three-parameter Gompertz models ($F = 29.840$, $p = 0.031$).

In comparison, the kinetic parameters are consistent with those reported by Chávez-Parga *et al.* (2008) in an Airlift bioreactor, suggesting that when scaling up the system, the kinetic constants could remain within similar ranges. However, the magnitude of these parameters may vary depending on the air flow rate and the type of diffuser, factors that directly influence oxygen transfer and mycelial morphology.

Since bikaverin is secreted into the extracellular medium, it is reasonable to assume that during prolonged cultivation the fungus or secreted enzymes could metabolize or degrade the pigment, leading to a decline in its apparent concentration. In our experiments, the available nitrogen was depleted before 24 h, a condition known to trigger metabolic shifts and to regulate the onset of secondary metabolism in *G. fujikuroi* and other filamentous fungi. Nitrogen limitation has been widely reported as a key signal controlling secondary metabolite biosynthesis and degradation processes (Tudzynski *et al.,* 2014). Therefore, the cultivation time was limited to 96 h to avoid possible pigment reuptake or degradation, focusing the analysis on a reliable interval where bikaverin accumulation showed a consistent increasing trend.

Figure 6 shows the kinetics fitted to the three models, confirming that biomass reaches its maximum around 48 h, at which point the stationary phase begins. Finally, bikaverin production was analyzed using the Luedeking–Piret model, which describes product formation as the sum of a growth-associated fraction $\left(\alpha \frac{dX}{dt}\right)$ and a non-growth-associated fraction (βX). The obtained parameters ($\alpha = -72.28$; $\beta = 2.114$) indicate that bikaverin is a predominantly non-growth-associated metabolite. The negative value of α suggests that cell growth not only does not favor its synthesis but may even dilute the pigment concentration during the exponential phase. In contrast, the positive and high value of β confirms that bikaverin accumulates mainly during the stationary phase, consistent with the typical profile of secondary metabolites in filamentous fungi (Giordano & Domenech, 1999; Spraker *et al.,* 2018). These results are consistent with previous studies, which describe bikaverin as a secondary metabolite synthesized predominantly during the stationary phase and is strongly influenced by oxygen availability (Choi *et al*., 2020; Limón *et al*., 2023).

The obtained results show that the three-parameter Gompertz model more accurately describes the growth kinetics of *G. fujikuroi* under the evaluated experimental conditions, as it captures both the exponential phase and the stabilization, followed by a slight decrease in biomass at the end of the culture. This agrees with reports for other filamentous fungi producing secondary metabolites, where the stationary phase is associated with greater accumulation of polyketide products. The fitting capacity of the kinetic models, together with statistical verification through the F-test, reinforces the robustness of the analysis and provides a quantitative basis for interpreting the system dynamics. Nevertheless, since bikaverin is a secondary metabolite, its formation does not necessarily follow the same trend as biomass, making

it necessary to perform a specific analysis of the coupling between growth and production. In this sense, the Luedeking–Piret model was applied to evaluate the growth-associated or non-associated nature of bikaverin biosynthesis, which is presented in subsection 3.5.1.

3.5.1 Product formation kinetics (Luedeking-Piret model)

The relationship between cell growth and bikaverin synthesis was evaluated using the Luedeking–Piret model (Equation 8). This model differentiates the growth-associated production fraction (α) from the non-growth-associated fraction (β), providing a key tool to determine the nature of secondary metabolite biosynthesis in filamentous fungi.

From the data of experiment 12, conducted under controlled culture conditions (dextrose 50 g/L, NH_4Cl 0.75 g/L, KH_2PO_4 1 g/L, $MgSO_4$ 1 g/L, temperature 28 ± 1 °C, initial pH 3, aeration 1 vvm, orbital agitation 100 rpm, 10% inoculum), the parameters α and β were estimated by ordinary least squares, without intercept. The obtained values were α = –72.28 and β = 2.114, with an R^2 = 0.921 based on the dP/dt values. The negative α value indicates that biomass increase does not favor bikaverin production but exerts a diluting or inhibitory effect, In contrast, the positive and significant β value confirms that pigment formation occurs predominantly in a non-growth-associated manner.

This behavior is consistent with the typical profile of polyketide-type secondary metabolites, whose synthesis is activated during stationary or nutrient-stress phases rather than during active growth (Spraker *et al*., 2018; Medentsev & Akimenko, 1998). Similarly, Chávez-Parga *et al*. (2008) reported negative α values in bikaverin production within an Airlift bioreactor, which was interpreted as a clear indication that biosynthesis is triggered by regulatory mechanisms rather than biomass expansion. Likewise, Wiemann *et al*. (2009) demonstrated that the expression of *bik* genes responsible for the biosynthetic pathway is induced under acidic pH and nitrogen-limiting conditions, which is consistent with the conditions evaluated in this study.

Figure 7 shows the model fitting to the experimental bikaverin concentration data, where the prediction aligns with the experimental trend, although with slight deviations at early times, attributable to the negative α value. This effect reinforces the idea that bikaverin production intensifies once limiting nutrients are depleted, confirming its nature as a secondary metabolite independent of growth.

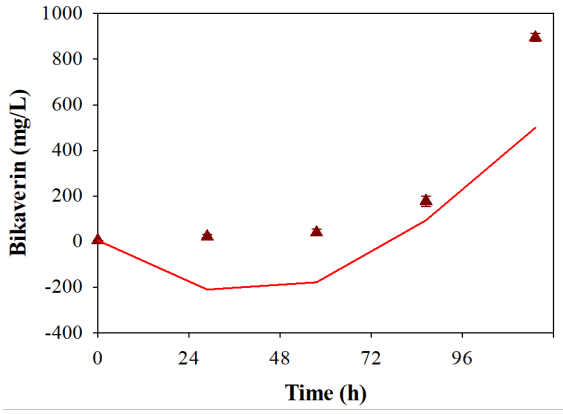

Figure 7. Bikaverin production profile by *G. fujikuroi* CDBB-H-972 under controlled conditions (initial pH 3, aeration 1 vvm, orbital agitation 100 rpm, temperature 28 ± 1 °C). (▲) Bikaverin concentration (mean ± SD, n = 2), while the solid line represents the fit of the Luedeking–Piret model (α = –72.28, β = 2.114).

Taken together, these results provide strong evidence that bikaverin in *G. fujikuroi* should be considered a strictly secondary metabolite, whose accumulation can be enhanced through culture-control strategies aimed at prolonging the stationary phase or intensifying stress conditions (e.g., dynamic pH control or variations in aeration rate). These findings are relevant for process scale-up design, as they enable the formulation of optimization strategies focus on maximizing pigment production beyond merely increasing biomass. The results confirm that bikaverin behaves as a non-growth-associated secondary metabolite, consistent with reports for other industrially relevant fungal polyketides. This result supports the applicability of the Luedeking–Piret model for describing production kinetics and emphasizes the relevance of regulating culture phases to enhance pigment accumulation. Once the formation kinetics were understood, the next key step involved the extraction and purification of the produced bikaverin to obtain the compound in crystalline form and proceed with its structural characterization, which confirmed its identity and allowed evaluation of the quality of the recovered metabolite.

3.6 Extraction and purification of produced bikaverin

Solid–liquid extractions were performed from the culture of *G. fujikuroi* CDBB-H-972, followed by concentration of the crude extract using a rotary evaporator. Subsequently, four successive washes with chloroform were performed, yielding extracts of varying color intensities depending on the cultivation time. Figure 8 shows the organic extracts collected from 0 to 96 hours, where a clear increase in pigment concentration is observed throughout the fermentation

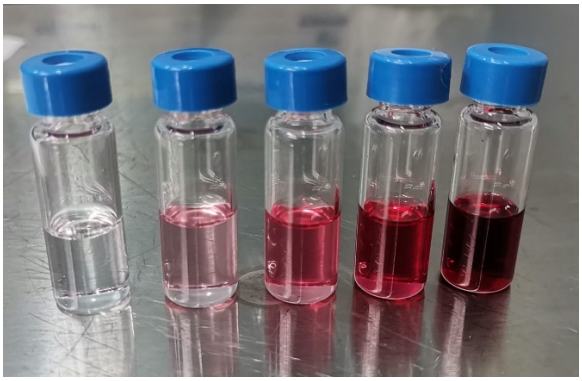

Figure 8. Organic phase extracts of *G. fujikuroi* CDBB-H-972 from 0 to 96 hours of cultivation.

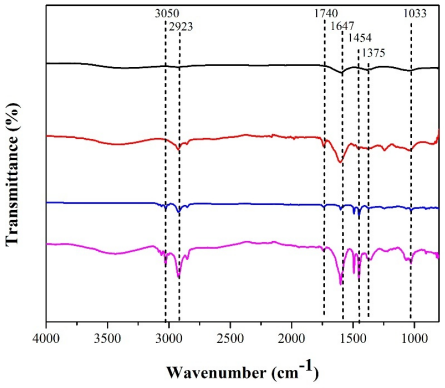

Figure 9. FTIR spectrum of (—) KBr pellet, (—) Bikaverin standard, (—) Chloroform, (—) Fraction 4 Bikaverin purified.

process. This gradient confirms that the highest proportion of bikaverin is associated with the biomass, validating its nature as an intracellular metabolite.

After purification of the crude extract, the characteristic red pigmentation allowed the visualization of distinct chromatographic bands. For the mobile phase employed, a retention factor (Rf) defined as the ratio between the distance traveled by the compound and that traveled by the solvent front of 0.85 was obtained, consistent with the association of bikaverin with cellular biomass and confirming its intracellular nature.

The crude fraction was purified by column chromatography on silica gel 60 acidified with oxalic acid (95:5, w/w), using a mobile phase consisting of a mixture of chloroform, methanol, and acetic acid (94:1:5, v/v/v). Thin-layer chromatography (TLC) analysis revealed an intense red band with an Rf value of 0.85, matching the commercial bikaverin standard (Sigma-Aldrich®). Structural characterization of the purified fraction was performed by FT-IR spectroscopy, and the results are shown in Figure 9.

The obtained spectra correspond to the characteristic peaks previously described for this polyketide, confirming the identity of the produced bikaverin.

A characteristic band was observed in the IR spectrum at 3050 cm^{-1}, characteristic of aromatic C–H stretching, 2923 cm^{-1} for unsaturated C–H groups, 1740 cm^{-1} for the C=O group, 1647 cm^{-1} for the C=C group, 1454 and 1375 cm^{-1} for C–H, and 1033 cm^{-1} for the C–O group. Studies conducted by Soumya *et al*. (2018) reported a similar IR spectrum; however, they characterized a red pigment produced by the fermentation of *Fusarium chlamydosporum*. Through SEM analysis, a more evident mycelial organization was observed, composed of loosely arranged hyphal filaments, hyphal aggregates forming mycelial strands, and some interconnections through anastomosis (Figure 10).

In the SEM micrographs, amorphous structures adhered to the mycelial surface were observed, showing morphology and distribution compatible with intracellular deposits. These aggregates could correspond to bikaverin accumulations, which have been previously reported as being either secreted or accumulated in specific regions of the mycelium. Cornforth *et al.* (1971) described bikaverin as a fungal vacuolization factor, owing to its possible role in inducing senescence-related morphological changes.

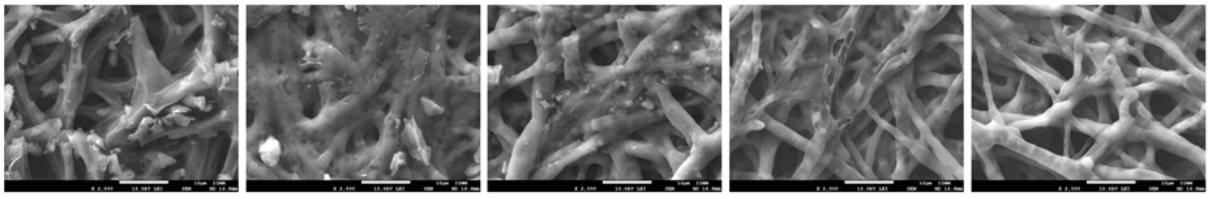

Figure 10. Scanning Electron Microscopy (SEM) analysis of *G. fujikuroi* CDBB-H-972 at 2500× magnification.

Conclusions

The results of this study provide clear evidence that *G. fujikuroi* efficiently produces bikaverin under controlled culture conditions, primarily influenced by the initial pH and aeration rate, with strain CDBB-H-972 exhibiting the best productive performance. The applied kinetic models confirmed that bikaverin production follows a non-growth-associated pattern, consistent with its classification as a secondary metabolite. Morphological analysis revealed structural alterations in the mycelium and intracellular pigment accumulation, in agreement with previous reports on fungal polyketides. Furthermore, the extraction, purification, and FT-IR characterization validated the identity of the metabolite, confirming the reliability of the experimental procedure. Overall, these findings provide valuable insights into the physiological and kinetic regulation of bikaverin biosynthesis, establishing a solid foundation for future optimization and scale-up efforts aimed at its biotechnological and pharmaceutical exploitation.

Acknowledgements

The authors acknowledge the financial support provided by the Secretaría de Ciencia, Humanidades, Tecnología e Innovación (SECIHTI) through the Doctoral Scholarship in Chemical Engineering Sciences (CVU No. 1081080). Appreciation is also extended to the Biotechnology and Bioengineering Laboratory of the Universidad Michoacana de San Nicolás de Hidalgo for the infrastructure and facilities that made this study possible.

Nomenclature

Y	Response variable of the experimental design
β_n	Estimated regression coefficients
OTR	Oxygen Transfer Rate, $mg\ O_2/Lh$
OUR	Oxygen Uptake Rate, $mg\ O_2/Lh$
Q_{O_2}	Oxygen Consumption rate, $mg\ O_2/Lh$
X	Biomass concentration, g/L
t_n	Time, s
a, k	Kinetics constants
f	Distribution coefficient
RSS_1	Residual sum of squares
DF_2	Degrees of freedom
P	Concentration of product, g/L.
α, β	Luedeking-Piret parameters
k_La	The mass transfer coefficient, h^{-1}
μ	Specific growth rate, h^{-1}
$Y_{\frac{X}{S}}$	Yield Biomass/substrate, $g\ biomass/g\ substrate$
$Y_{\frac{P}{X}}$	Yield Product/Biomass, $g\ product/g\ biomass$
vvm	Aeration rate, volume of air per volume of medium per minute
rpm	Orbital agitation, revolutions per minute

References

Amaral, P. F. F., Freire, M. G., Rocha-Leão, M. H. M., Marrucho, I. M., Coutinho, J. A. P., & Coelho, M. A. Z. (2008). Optimization of oxygen mass transfer in a multiphase bioreactor with perfluorodecalin as a second liquid phase. *Biotechnology and Bioengineering*, *99*(3), 588–598. https://doi.org/10.1002/bit.21640

Anama, Y. P., Díaz, R., Duarte-Alvarado, D. E., & Lagos-Burbano, T. C. (2021). Morphological and pathogenic characterization of *Fusarium oxysporum* in lulo (Solanum spp.). *Revista de Ciencias Agrícolas*, *38*(1), 20–37. https://doi.org/10.22267/rcia.213801.142

Bailey, J. E., & Ollis, D. F. (1977). *Biochemical Engineering Fundamentals*. Editorial McGraw-Hill, 2nd ed. United States

Balan, J., Fuska, J., Kuhr, I., & Kuhrová, V. (1970). Bikaverin, an antibiotic from *Gibberella fujikuroi*, effective against *Leishmania brasiliensis*. *Folia Microbiologica*, *15*(6), 479–484. https://doi.org/10.1007/BF02880192

Borkertas, S., Viskelis, J., Viskelis, P., Streimikyte, P., Gasiunaite, U., & Urbonaviciene, D. (2025). Fungal Biomass Fermentation: Valorizing the Food Industry's Waste. *Fermentation*, *11*(6), 351. https://doi.org/10.3390/fermentation11060351

Chávez-Parga, M. del C., González-Ortega, O., Negrete-Rodríguez, M. de la L. X., Vallarino, I. G., Alatorre, G. G., & Escamilla-Silva, E. M. (2008). Kinetic of the gibberellic acid and bikaverin production in an airlift bioreactor. *Process Biochemistry*, *43*(8), 855–860. https://doi.org/10.1016/J.PROCBIO.2008.04.007

Chávez-Parga, M. C., Hinojosa-Ventura, G., Maya-Yescas, R., & González-Hernández, J. C. (2014). Effect of rates of aeration and agitation on the volumetric coefficient of oxygen transfer in the production of bikaverin. *International Review Of Chemical Engineering (IRECHE)*, *6*(2), 100-107.

Chisti, Y. (2016). Airlift bioreactors: Principles, applications, and recent advances. *Chemical Engineering and Processing: Process Intensification*, 104, 1–21. https://doi.org/10.1016/j.cep.2016.03.007

Choi, S., Lee, S., Kim, J., & Park, Y. (2020). Regulation of bikaverin biosynthesis and oxidative metabolism in *Fusarium fujikuroi* under oxygen-limited fermentation. Journal of Biotechnology, 318, 45–53. https://doi.org/10.1016/j.jbiotec.2020.07.012

Cornforth, J. W., Ryback, G., Robinson, P. M., & Park, D. (1971). Isolation and characterization of a fungal vacuolation factor (bikaverin). *Journal of the Chemical Society C: Organic*, 2786. https://doi.org/10.1039/j39710002786

Doran, P. M. (2013). *Bioprocess engineering principles*. Academic Press. United Kingdom

Garza-Garza, C., Olguin-Maciel, E., Valdez-Ojeda, R., Huchin-Poot, E., Toledano-Thompson, T., Azcorra-May, K., Alzate-Gaviria, L., Dominguez-Maldonado, J., Lappe-Oliveras, P., & Tapia-Tussell, R. (2025). Bio-saccharification and fermentation process of a non-conventional starchy material with isolates of autochthonous strains. Revista Mexicana de Ingeniería Química, 24(2), 1-26. https://doi.org/10.24275/rmiq/bio25497

Giordano, W., & Domenech, C. E. (1999). Aeration affects acetate destination in *Gibberella fujikuroi*. *FEMS Microbiology Letters*, *180*(1), 111–116. https://doi.org/10.1111/j.1574-6968.1999.tb08784.x

Hinojosa Ventura, G., Puebla Pérez, A. M., Gallegos Arreola, M. P., Chávez Parga, M. del C., Romero Estrada, A., & Delgado Saucedo, J. I. (2019). Cytotoxic and Antitumoral Effects of Bikaverin from *Gibberella fujikuroi* on L5178Y Lymphoma Murine Model. *Journal of the Mexican Chemical Society*, *63*(4). https://doi.org/10.29356/jmcs.v63i4.729

Leslie, J. F., & Summerell, B. A. (2006). The Fusarium Laboratory Manual. En *Wiley eBooks*. https://doi.org/10.1002/9780470278376

Limón, M. C., Rodríguez-Ortiz, R., & Avalos, J. (2023). Oxygen availability modulates bikaverin production and fungal differentiation in *Fusarium fujikuroi*. *Applied Microbiology and Biotechnology*, 107(5), 1911–1924. https://doi.org/10.1007/s00253-023-12215-2

Limón, M. C., Rodríguez-Ortiz, R., & Avalos, J. (2010). Bikaverin production and applications. *Applied Microbiology and Biotechnology*, *87*(1), 21–29. https://doi.org/10.1007/s00253-010-2551-1

Lu, H., Guo, S., Yang, Y., Zhao, Z., Xie, Q., Wu, Q., Sun, C., Luo, H., An, B., & Wang, Q. (2025). Bikaverin as a molecular weapon: enhancing *Fusarium oxysporum* pathogenicity in bananas via rhizosphere microbiome manipulation. *Microbiome*, *13*(1). https://doi.org/10.1186/s40168-025-02109-7

Machado, S., Feitosa, V., Pillaca-Pullo, O., Lario, L., Sette, L., Pessoa, A., & Alves, H. (2022). Effects of oxygen transference on protease production by *Rhodotorula mucilaginosa* CBMAI 1528 in a stirred tank bioreactor. *Bioengineering*, *9*(11), 694. https://doi.org/10.3390/bioengineering9110694

Martínez-Moreno, F., Jofre y Garfias, A. E., Hernández-Orihuela, A. L., & Martínez-Antonio, A. (2021). Avocado seed hydrolysate as an alternative growth medium for fungi. *Revista Mexicana de Ingeniería Química*, *20*(2), 569–580. https://doi.org/10.24275/rmiq/Bio1951

Medentsev, A. G., Arinbasarova, A. Yu., & Akimenko, V. K. (2005). Biosynthesis of Naphthoquinone Pigments by Fungi of the Genus *Fusarium*. *Applied Biochemistry and Microbiology*, *41*(5), 503–507. https://doi.org/10.1007/s10438-005-0091-8

Medentsev, A., & Akimenko, V. (1998). Naphthoquinone metabolites of the fungi. Phytochemistry, 47(6), 935-959. https://doi.org/10.1016/s0031-9422(98)80053-8

Miller, G. L. (1959). Use of Dinitrosalicylic Acid Reagent for Determination of Reducing Sugar. *Analytical Chemistry*, *31*(3), 426–428. https://doi.org/10.1021/ac60147a030

Nirmaladevi, D., Venkataramana, M., Chandranayaka, S., Ramesha, A., Jameel, N. M., & Srinivas, C. (2014). Neuroprotective Effects of Bikaverin on H2O2-Induced Oxidative Stress Mediated Neuronal Damage in SH-SY5Y Cell Line. *Cellular and Molecular Neurobiology*, *34*(7), 973–985. https://doi.org/10.1007/s10571-014-0073-6

Santiago da Silva, W. (2013). *¨Produção de pigmentos fúngicos e seu uso no tingimento de tecidos* Tesis Maestre Dissertação apresentada ao programa de Pós Graduação em Tecnologias para

o Desenvolvimento Sustentável. Universidade Federal de São João Del-Rei (UFSJ). Brasil.

Santos, M. C. D., De Lima Mendonça, M., & Bicas, J. L. (2020). Modeling bikaverin production by *Fusarium oxysporum* CCT7620 in shake flask cultures. *Bioresources And Bioprocessing*, *7*(1). https://doi.org/10.1186/s40643-020-0301-5

Solórzano, L. (1969). Determination of Ammonia in natural waters by the Phenolhypochlorite Method 1 1 This research was fully supported by U.S. Atomic Energy Commission Contract No. ATS (11-1) GEN 10, P.A. 20. *Limnology and Oceanography*, *14*(5), 799–801. https://doi.org/10.4319/lo.1969.14.5.0799

Soumya, K., Narasimha Murthy, K., Sreelatha, G. L., & Tirumale, S. (2018). Characterization of a red pigment from *Fusarium chlamydosporum* exhibiting selective cytotoxicity against human breast cancer MCF-7 cell lines. *Journal of Applied Microbiology*, *125*(1), 148–158. https://doi.org/10.1111/jam.13756

Spraker, J. E., Wiemann, P., Baccile, J. A., Venkatesh, N., Schumacher, J., Schroeder, F. C., Sanchez, L. M., & Keller, N. P. (2018). Conserved Responses in a War of Small Molecules between a Plant-Pathogenic Bacterium and Fungi. *mBio*, *9*(3). https://doi.org/10.1128/mbio.00820-18

Tudzynski, B. (2014). Nitrogen regulation of fungal secondary metabolism in fungi. *Frontiers In Microbiology*, *5*. https://doi.org/10.3389/fmicb.2014.00656

Valle, P., Salazar, Y., Soto-Cruz, N., Páez-Lerma, J., Coria, L., Núñez-Guerrero, M., Rodríguez-Herrera, R., & Herrera, L. (2024). Modelling and analysis on the ethanol production by the *Torulaspora delbrueckii* yeast. *Revista Mexicana de Ingeniería Química*, *23*(3), 1-17. https://doi.org/10.24275/rmiq/sim24312

Wiemann, P., Willmann, A., Straeten, M., Kleigrewe, K., Beyer, M., Humpf, H., & Tudzynski, B. (2009). Biosynthesis of the red pigment bikaverin in *Fusarium fujikuroi*: genes, their function and regulation. *Molecular Microbiology*, *72*(4), 931–946. https://doi.org/10.1111/j.1365-2958.2009.06695.x

Zwietering, M. H., Jongenburger, I., Rombouts, F. M., & van 't Riet, K. (1990). Modeling of the Bacterial Growth Curve. *Applied and Environmental Microbiology*, *56*(6), 1875–1881. https://doi.org/10.1128/aem.56.6.1875-1881.1990